Chemical sensors based on Periodic Mesoporous Organosilica @ $NaYF_4$: Ln^{3+} nanocomposites

Wanlu Liu,[a, b, c] *Anna M. Kaczmarek,*[b] Pascal Van Der Voort,*[c] *and Rik Van Deun*[a]*

[a] L^3 – Luminescent Lanthanide Lab, Department of Chemistry, Ghent University, Krijgslaan 281-S3, 9000 Ghent, Belgium.

[b] NanoSensing Group, Department of Chemistry, Ghent University, Krijgslaan 281-S3, 9000 Ghent, Belgium.

[c] Center for Ordered Materials, Organometallics and Catalysis (COMOC), Department of Chemistry, Ghent University, Krijgslaan 281-S3, 9000 Ghent, Belgium.

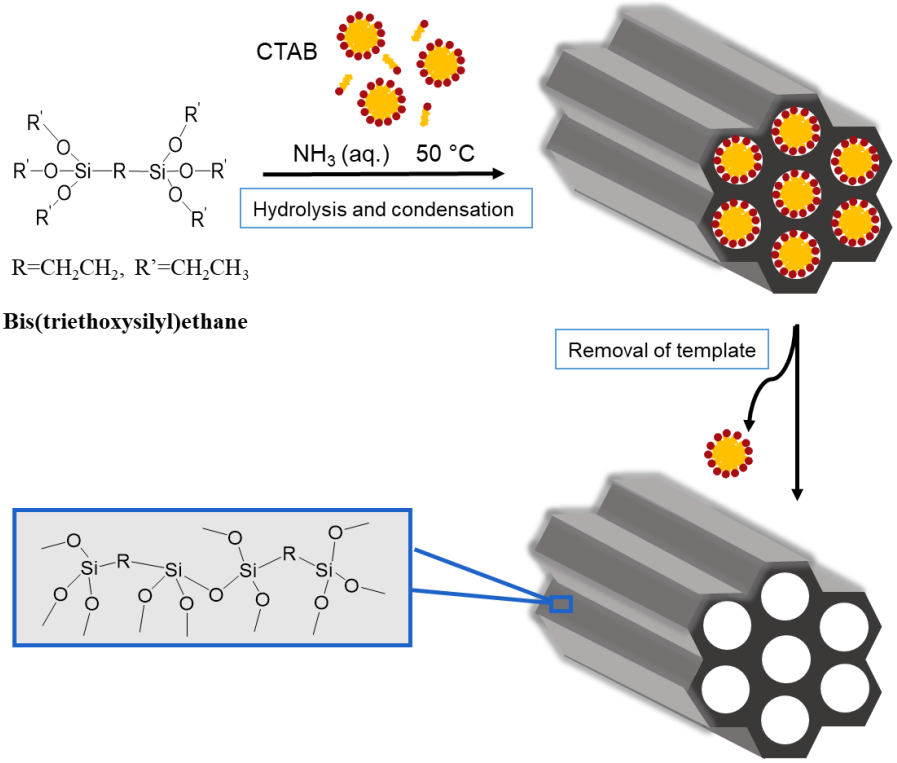

Scheme S1. Synthesis route of ethane PMO nanoparticles.

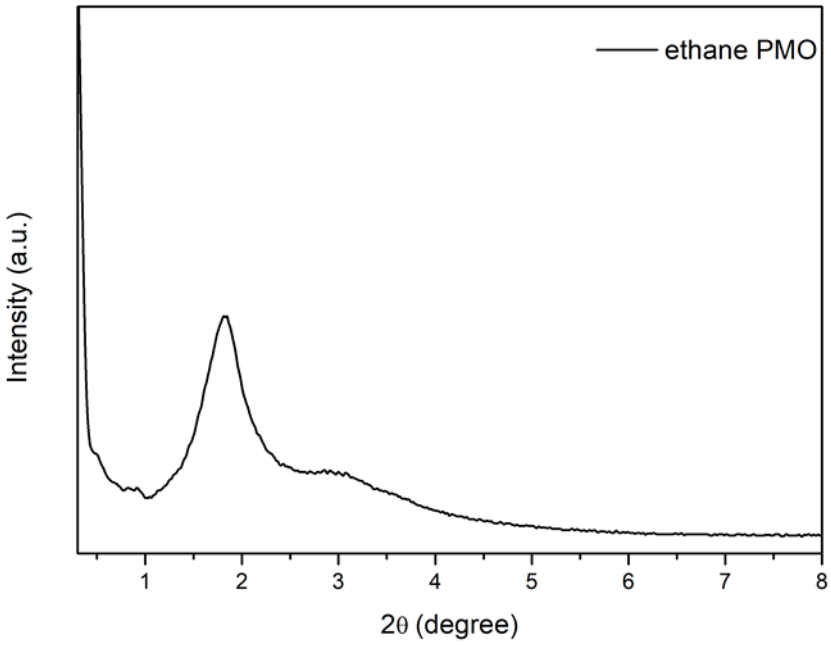

Figure S1. Powder XRD pattern of ethane PMO used for the preparation of PMO@$NaYF_4$: Yb^{3+}, Ln^{3+} (Ln =Er, Tm, Ho) nanocomposites.

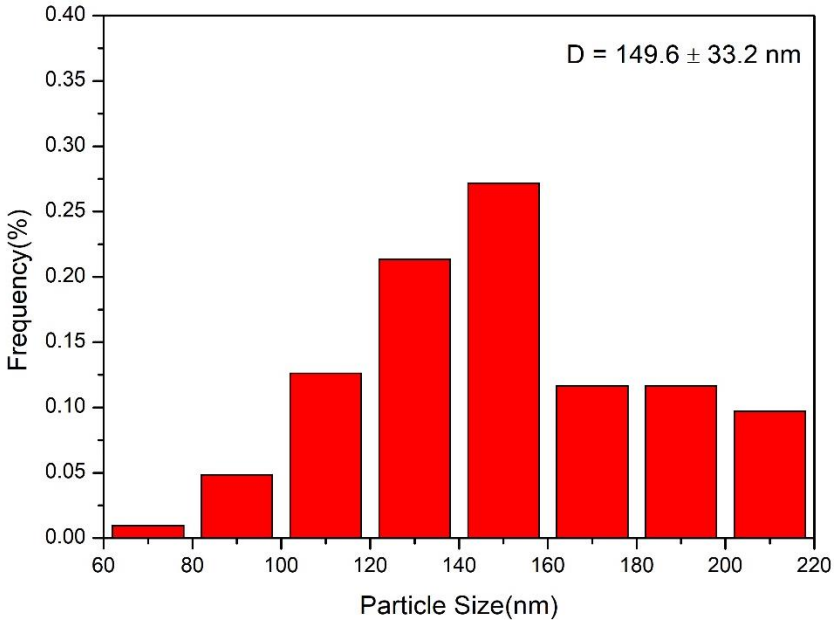

Figure S2. Particle size distribution diagram of ethane PMO nanoparticles.

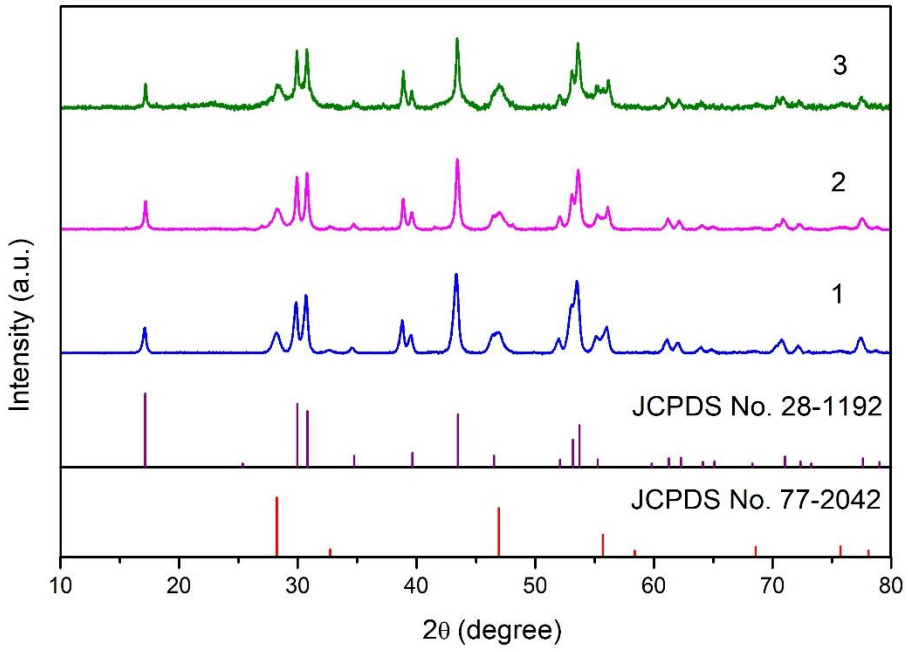

Figure S3. Powder XRD patterns of PMO@$NaYF_4$: Yb^{3+}, Ho^{3+} synthesized three times under the same synthesis conditions.

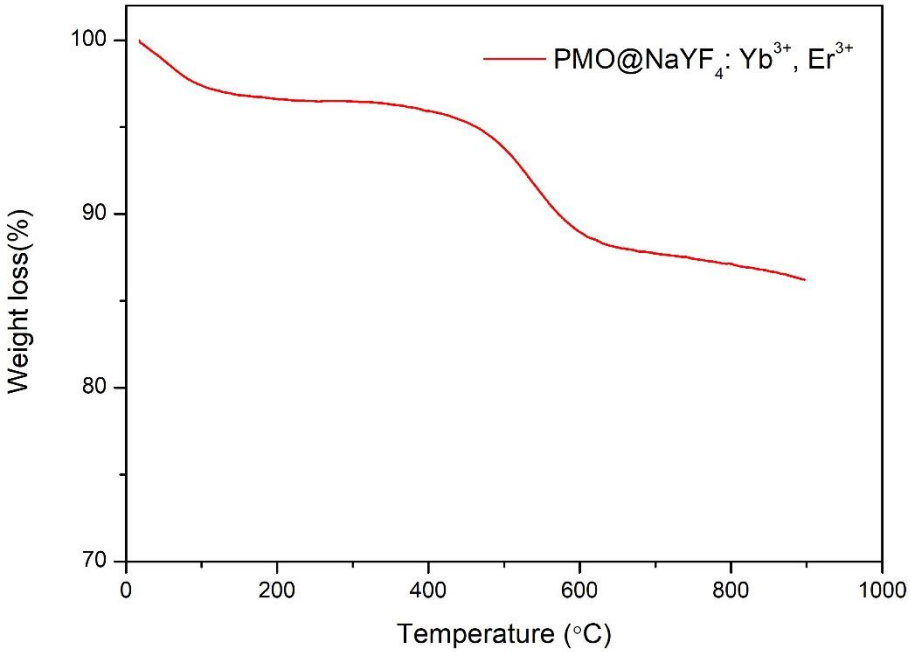

Figure S4. Thermogravimetric analysis of PMO@$NaYF_4$: Yb^{3+}, Er^{3+}.

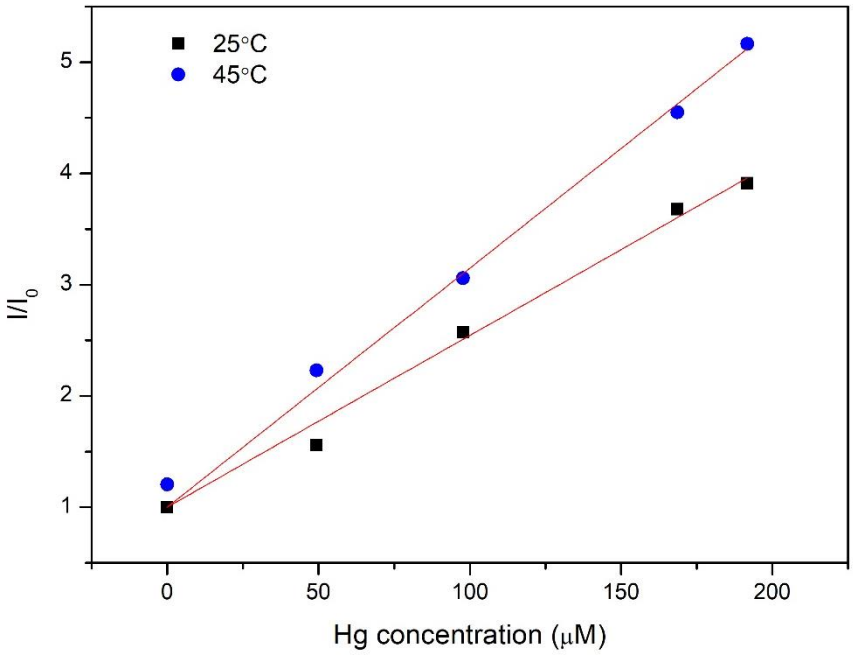

Figure S5. The Stern-Volmer plots of PMO@$NaYF_4$: Yb^{3+}, Er^{3+} in the presence of Hg^{2+} ions at different temperatures (25 ºC and 45 ºC). An increase of the slope with temperature increase suggests presence of dynamic quenching mechanism.

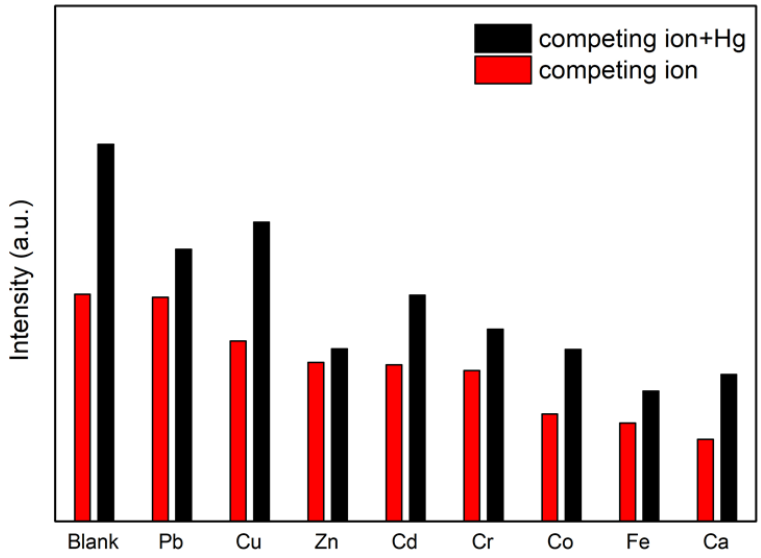

Figure S6. Luminescence emission intensity of PMO@$NaYF_4$: Yb^{3+}, Er^{3+} in the presence of a single competing ion (red bars) and in the mixture of Hg^{2+} and competing ions (black bars).

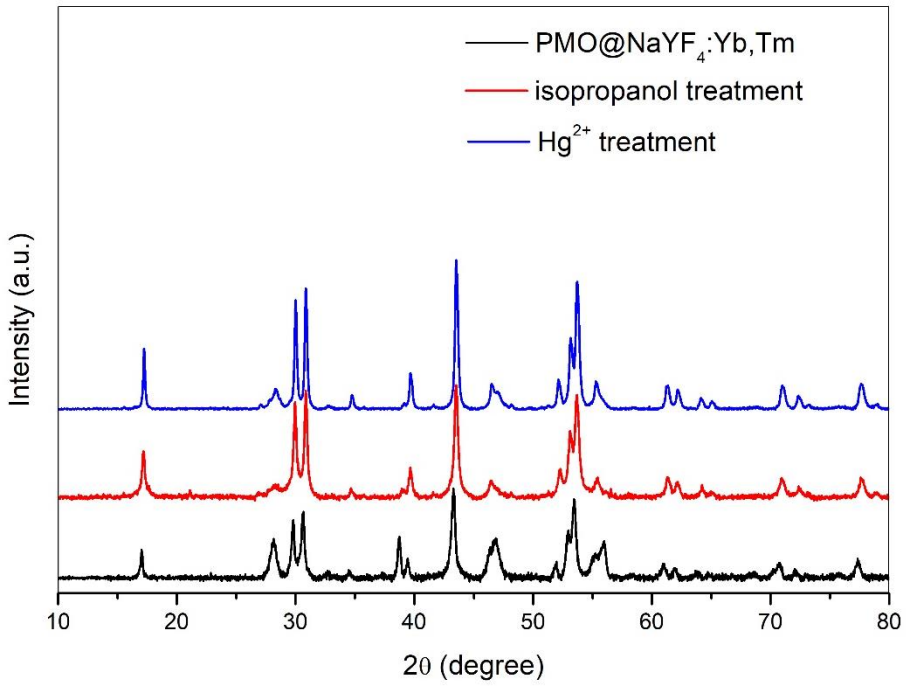

Figure S7. Combined powder XRD patterns of PMO@$NaYF_4$: Yb^{3+}, Tm^{3+} before and after sensing experiments.

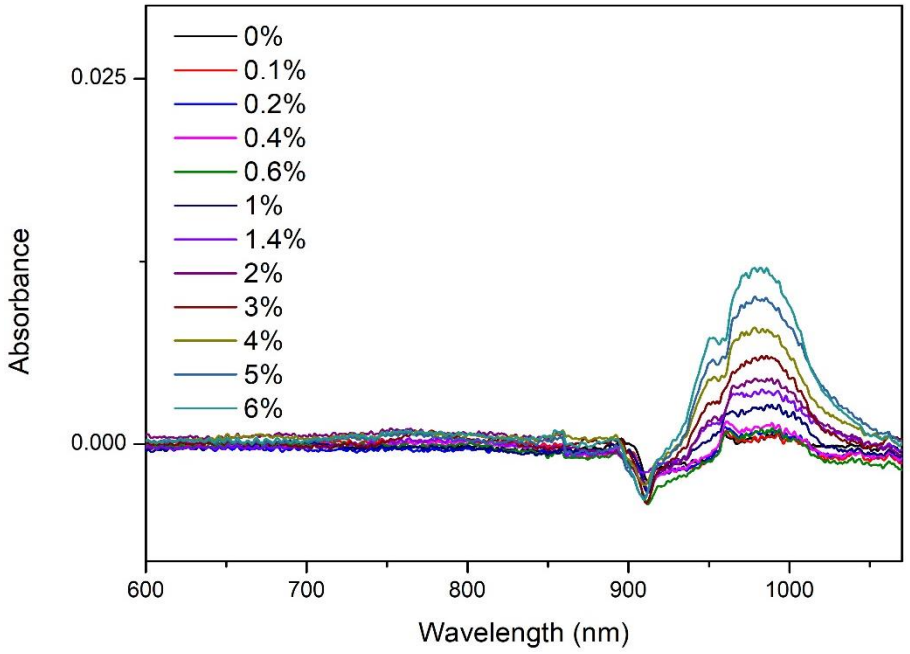

Figure S8. Absorption spectra of isopropanol containing varied water content.

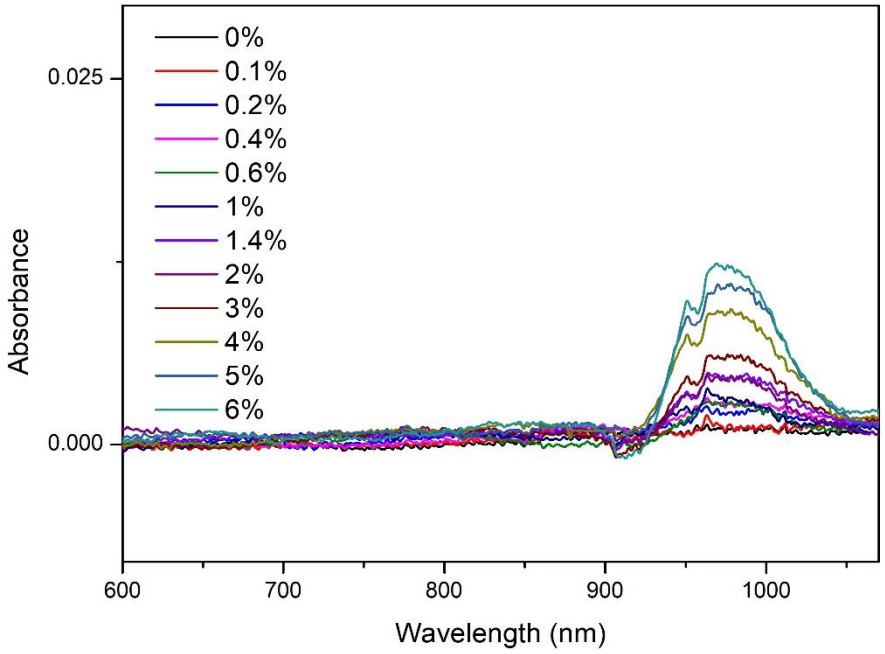

Figure S9. Absorption spectra of n-butanol containing varied water content.

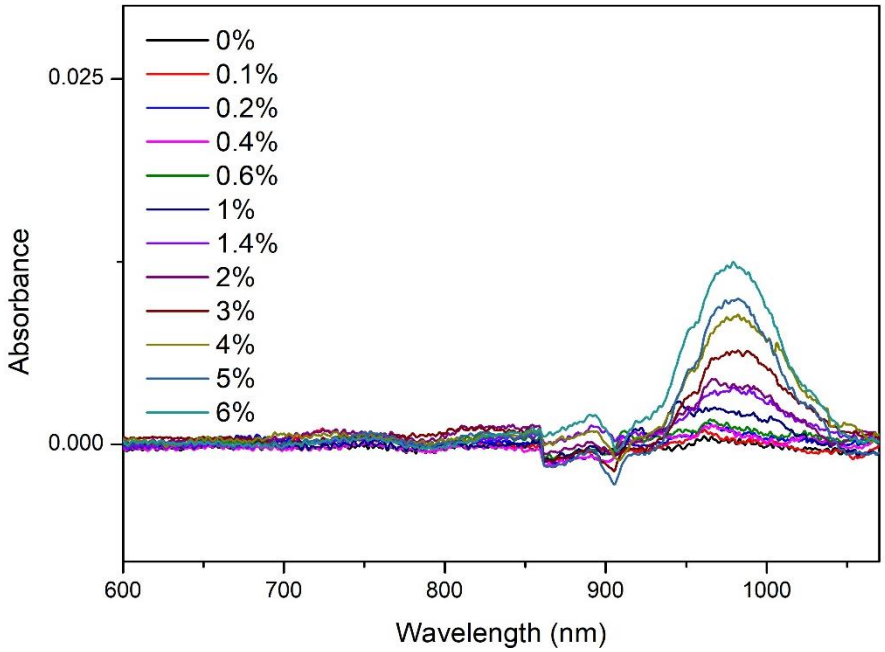

Figure S10. Absorption spectra of ethanol containing varied water content.

Table S1. Comparison of various upconverison luminescence sensors for Hg^{2+}detection

Sensors	Structure property	Need to pre-synthesize UCNPs?	Linear range (μM)	Limit of detection (μM)	Ref.
A-DMSA-UCNPs	Core-Shell	Yes	24-120	2.47	1
A-PAA-UCNPs	Core-Shell	Yes	13.4-40	8.15	1
Ru-UCNP@HmSiO$_2$-PEI	Core-Shell	Yes	0-46	0.16	2
UCNPs-aptamers-GNPs	Mixture	Yes	0.2-20	0.06	3
UCNP/ QDs	Composites	Yes	0.01-2.8	0.015	4
PMO@NaYF$_4$: Yb^{3+}, Er^{3+}	Composites;	No	0-214.6	24.4	This

	porous				work

Table S2. Comparison of various materials for determination of water content in organic solvents

Sensors	Measured media	Linear range (v/v)	Limit of detection (v/v)	Ref.
Lignin-derived red-emitting CDs	Ethanol	10-60%	0.36	5
MOF:Tb	Ethanol	0-11.76%	1.12%	6
FS@ZIF-9/Co-formate	Ethanol isopropanol	0-10%	0.43% 0.63%	7
Eu^{3+}@UiO-66-NH_2-IM	Ethanol	0-2%	0.088%	8
PMO@$NaYF_4$: Yb^{3+}, Er^{3+}	Isopropanol n-butanol	0-0.75%	0.21% 0.18%	This work
PMO@$NaYF_4$: Yb^{3+}, Ho^{3+}	Ethanol	0-0.75%	0.29%	This work

References

1 C. Yang, Y. Li, N. Wu, Y. Zhang, W. Feng, M. Yu and Z. Li, *Sens. Actuators, B*, 2021, **326**, 128841.

2 X. Ge, L. Sun, B. Ma, D. Jin, L. Dong, L. Shi, N. Li, H. Chen and W. Huang, *Nanoscale*, 2015, **7**, 13877-13887.

3 Y. Liu, Q. Ouyang, H. Li, M. Chen, Z. Zhang and Q. Chen, *J. Agric. Food Chem.*, 2018, **66**, 6188-6195.

4 S. Cui, S. Xu, H. Song, W. Xu, X. Chen, D. Zhou, Z. Yin and W. Han, *RSC Adv.*, 2015, **5**, 99099-99106.

5 J. Wang, J. Wang, W. Xiao, Z. Geng, D. Tan, L. Wei, J. Li, L. Xue, X. Wang and J. Zhu, *Anal. Methods*, 2020, **12**, 3218-3224.

6 P. Majee, P. Daga, D. K. Singha, D. Saha, P. Mahata and S. K. Mondal, *J. Photochem. Photobiol., A*, 2020, **402**, 112830.

7 X. Zhao, M. Zheng, Y. Zhao, T. Wang, J. Li, Z. Xie, Y. Zhang, Z. Liu, X. Wang, Z. Gao and H. Huang, *Microporous Mesoporous Mater.*, 2019, **290**, 109624.

8 S.-Y. Zhu and B. Yan, *Ind. Eng. Chem. Res.*, 2018, **57**, 16564-16571.